

Fluctuations in Polymer Translocation

P. L. Krapivsky¹ and K. Mallick²

¹ *Department of Physics, Boston University, Boston, MA 02215, USA*

² *Institut de Physique Théorique CEA, IPhT, F-91191 Gif-sur-Yvette, France*

We investigate a model of chaperone-assisted polymer translocation through a nanopore in a membrane. Translocation is driven by irreversible random sequential absorption of chaperone proteins that bind to the polymer on one side of the membrane. The proteins are larger than the pore and hence the backward motion of the polymer is inhibited. This mechanism rectifies Brownian fluctuations and results in an effective force that drags the polymer in a preferred direction. The translocated polymer undergoes an effective biased random walk and we compute the corresponding diffusion constant. Our methods allow us to determine the large deviation function which, in addition to velocity and diffusion constant, contains the entire statistics of the translocated length.

PACS numbers: 05.60.-k, 87.16.Ac, 05.10.Ln

Keywords: Translocation, Ratchet Effect, Non-Equilibrium Fluctuations

Proteins, nucleic acids, and various products synthesized inside cells are transported within the cytoplasm by molecular machines or motors [1]. Polymeric chains may also translocate in order to get in or out of organelles within the cell, or to cross the cell's outer membrane [2]. Both transport and translocation cannot rely on diffusion alone: macromolecules are subject to thermal fluctuations which are isotropic and from which, according to the second law of thermodynamics, no useful work can be extracted. Pure diffusion can account neither for the directionality of motion nor for the observed time scales — supplementary mechanisms that induce active and directed motion must be taken into account. The 'Brownian Ratchet' [3] provides a general setting to describe rectification of diffusive motion using chemical energy. This paradigm helps to understand the physics of molecular motors and to construct mathematical models of the translocation process. As explained e.g. in Refs. [4, 5], Brownian motion will cause a protein undergoing the translocation through the pore to fluctuate back and forth, and chemical asymmetries will rectify its displacement. Several mechanisms [6] can play this role including, for instance, disulfide bond formation, attachment of sugar bonds, binding of chaperone proteins on one side of the membrane. These rectification processes induce an effective force on the polymeric chain that drags it in the desired direction by inhibiting backwards motion.

The chaperone-assisted translocation [4, 5, 7–12] is a common mechanism for protein translocation and perhaps for DNA transport through membranes [13]. Earlier work [4, 5, 7, 10] has focused on continuous space and time descriptions. This assumption effectively means that the chaperone molecule is much longer than the lattice size. In the case of nucleic acids, for instance, the lattice size is the interbase distance ~ 0.36 nm which is about 6 times shorter than the chaperone molecule. Hence the discreteness of the monomers which are the binding sites for the chaperones can have sizable effect on the kinetics of the process. D'Orsogna, Chou, and Antal [12] have recently investigated a discrete model of the polymer translocation driven by the irreversible random sequential absorption of chaperone proteins on one side of the pore. The chief analytical result of Ref. [12] is the computation of the translocation velocity. Needless to say, the translocation velocity (here, the average translocated length per unit time) provides a partial description which is not sufficient in many biologically relevant cases, especially when the translocated polymers are not too long. In these situations dispersion (quantified by diffusion coefficients) and more generally large deviations play an important role. The goal of the present work is to carry out a thorough mathematical analysis of this polymer translocation model. We shall focus on the diffusion coefficient, although our approach gives the full statistics of the translocated length, for instance all its higher cumulants.

The outline of this work is as follows. In section I, we describe the translocation model and discuss some of its general scaling properties. In section II, we investigate the simplest case when chaperone molecules attach to single monomers along the polymer chain. First, we calculate the velocity as a function of the parameters of the model. Then we determine the large deviation function which encodes the full statistics of the translocated length; in particular, the large deviation function contains the velocity and the diffusion constant. In section III, we study a continuous space model where the chaperones are free to bind anywhere on the translocated segment of the polymer. This corresponds to the limit when the size of the chaperone molecule is large with respect to the monomer size (providing the natural minimal size in the problem, the lattice spacing). In this continuum case the velocity and the fluctuations can also be determined analytically. We show that the predictions of the discrete and the continuum frameworks match when the chaperon attachment rate λ is vanishingly small. In the complimentary limit of large attachment rate, the system becomes equivalent to a continuous time random walk. This limit admits a separate more elementary analysis and it provides a useful check of the consistency of our calculations. Finally in section IV we discuss possible extensions. A generalization to the situation when the polymer undergoes a bias diffusion and various technical calculations are relegated to Appendices.

I. GENERAL DESCRIPTION OF THE SYSTEM

Consider a polymer chain that passes through a pore in a membrane (see figure 1). We assume that the motion of the polymer chain is equivalent to unbiased random walk, i.e., it is fully described by one parameter, the diffusion coefficient D . The pore is located at $x = 0$ and we focus on the polymer segment to the right of the membrane (the region located on the right-hand side of the pore is the *target region* of the translocation process). At a given moment, this polymer segment consists of a certain number L of monomer units, each of size a , labeled $1, \dots, L$. Translocation is reversible and the polymer can move by one-monomer unit to the right or left with equal rates, resulting in a zero average translocation velocity and a non-vanishing diffusion coefficient D for the ‘bare’ polymer. We now suppose that the medium on the right side of the membrane contains a fixed density of special molecules — “chaperones” — that adsorb irreversibly, with a certain rate λ , onto unoccupied adjacent sites of the polymer. A chaperone is sufficiently large that it cannot pass through the pore (Fig. 1). As a result, the chaperones rectify the polymer diffusion so that it passes through the pore at a non-zero speed v and has a certain effective diffusion coefficient \mathcal{D} . More precisely, L , the number of translocated monomers at time t , is a random variable. Let $P(L, t)$ be the corresponding probability distribution. One anticipates that this distribution is asymptotically Gaussian,

$$P(L, t) \rightarrow \frac{1}{\sqrt{4\pi\mathcal{D}t}} e^{-(L-vt)^2/4\mathcal{D}t}, \quad (1)$$

where the velocity and the diffusion coefficient of the tip characterize, respectively, the average and the variance of L

$$\langle L \rangle = vt, \quad \langle L^2 \rangle - \langle L \rangle^2 = 2\mathcal{D}t. \quad (2)$$

The quantities v and \mathcal{D} depend on λ , the length ℓ of the chaperone molecule, the monomer length a , and the bare diffusion coefficient D . On dimensional grounds, we can write

$$v = \frac{D}{\ell} F(\bar{\lambda}, \frac{\ell}{a}), \quad \mathcal{D} = D G(\bar{\lambda}, \frac{\ell}{a}) \quad \text{with} \quad \bar{\lambda} = \frac{\lambda\ell^3}{D}. \quad (3)$$

These simple relations predict scaling behaviors in the interesting regime of small adsorption rate, that is, when $\bar{\lambda} \ll 1$. In this limit we anticipate that the length of the chaperone molecules should become irrelevant. This implies that $F \sim \bar{\lambda}^{1/3}$ as $\bar{\lambda} \rightarrow 0$, while G remains finite. Therefore

$$v \sim \lambda^{1/3} D^{2/3} \quad \text{and} \quad \mathcal{D} \sim D \quad \text{when} \quad \bar{\lambda} = \frac{\lambda\ell^3}{D} \rightarrow 0. \quad (4)$$

In the opposite limit of large adsorption rate, $\bar{\lambda} \gg 1$, we anticipate that adsorption becomes irrelevant. This suggests that

$$v \sim \frac{D}{\ell} \quad \text{and} \quad \mathcal{D} \sim D \quad \text{when} \quad \bar{\lambda} = \frac{\lambda\ell^3}{D} \rightarrow \infty. \quad (5)$$

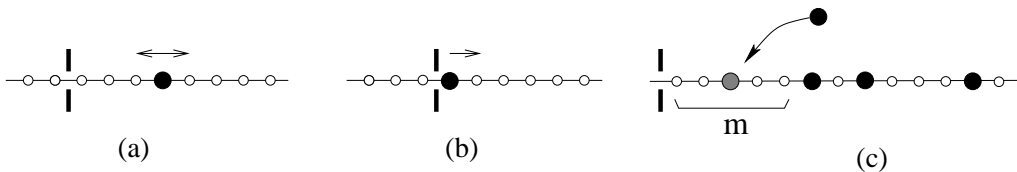


FIG. 1: Illustration of chaperon-assisted translocation. (a) The polymer can hop in either direction. (b) The polymer can hop only to the right because an adsorbed chaperone (large dot) is next to the pore (hole in the membrane barrier) and is too large to enter. (c) Adsorption of a new chaperone (shaded) at a site on the leftmost chaperone-free segment.

In the following sections we derive exact expressions for the functions $F(\bar{\lambda})$ and $G(\bar{\lambda})$ defined in Eq. (3). We will confirm the scaling behaviors of (4)–(5) and determine analytical expressions for the prefactors.

II. ANALYSIS OF THE DISCRETE SPACE MODEL

In this section we analyze the simplest discrete model corresponding to the situation when chaperone molecules have the same length as the monomer units of the polymer chain ($\ell = a$). Bound molecules do not overlap, that

is, there is at most one chaperone per site. Another assumption is that the binding of chaperone molecules to the polymer is irreversible. No other assumptions will be made and the following analysis will involve no approximations.

The polymer hops to the left and right with equal rates which we set equal to unity; we further set $\ell = 1$. With these agreements, the intrinsic diffusion constant D of the bare polymer is also equal to 1. Chaperones attach to empty sites with rate λ and we assume that attachment is irreversible (the detachment rate is 0). Since we set $\ell = 1$ and $D = 1$, the adsorption rate λ becomes dimensionless, $\lambda = \bar{\lambda}$.

At any given moment, the complete description is provided by the length L of the translocated segment of the polymer and the positions of the occupied monomers by adsorbed chaperones:

$$1 \leq m_1 < m_2 < \dots < m_M \leq L. \quad (6)$$

The length L of the translocated segment, the number M of the attached chaperone molecules (equivalently, the number of occupied monomers) and their positions m_1, \dots, m_M along the polymer chain are all random variables. At a given time, the first monomer to the right of the pore is always labeled as 1. The above definition (6) shows that an occupied monomer is not allowed to move to the position $x = 0$; in other words, if $m_1 = 1$ the segment can hop only to the right, while for $m_1 > 1$ both hops are equally possible. The full description requires the computation of the probability density $P(L; m_1, \dots, m_M; t)$. A shorter description ignores all monomers except the one closest to the pore, located at a certain site j (i.e. $m_1 = j$). In other words, this shorter description focuses on the segment probability $Q_j(t)$, namely the probability that at time t , the leftmost chaperone is located at distance j from the pore. Schematically,

$$Q_j(t) = \text{Prob}\{|\underbrace{\circ \dots \circ}_{j-1} \bullet\}$$

where the vertical line represents the position of the membrane pore. The key feature of this problem is that the time-evolution equations of the $Q_j(t)$'s form a closed set and can be solved. (For a review of techniques developed in studies of adsorption kinetics, see [14, 15].) These equations read

$$\frac{dQ_j(t)}{dt} = Q_{j-1}(t) + Q_{j+1}(t) + \lambda \sum_{k>j} Q_k(t) - [2 + \lambda(j-1)]Q_j(t) \quad \text{for } j > 1, \quad (7)$$

$$\frac{dQ_1(t)}{dt} = Q_2(t) + \lambda \sum_{k>1} Q_k(t) - Q_1(t). \quad (8)$$

The terms in Eqs. (7) are self-explanatory, e.g. the first two terms on the right-hand side describe the gain due to hopping, while the third gain term represents adsorption events. Equation (8) does not fully fit into the pattern, but if we add an extra variable $Q_0(t)$ with $Q_0(t) = Q_1(t)$, then equation (8) does take the same form as Eqs. (7). As a useful check of self-consistency one can add Eqs. (7)–(8) and verify that the sum $\sum_{k>0} Q_k(t)$ is conserved. (By normalization, $\sum_{k>0} Q_k(t) = 1$ must hold for all values of t .)

It is useful to define the cumulative variable $E_m(t) = \sum_{k>m} Q_k(t)$. Note that $Q_m(t) = E_{m-1}(t) - E_m(t)$. The quantities $E_m(t)$ represent empty interval probabilities

$$E_m(t) = \text{Prob}\{|\underbrace{\circ \dots \circ}_m\}.$$

In particular, we have $E_0(t) = \sum_{k>0} Q_k(t) = 1$ and $E_{-1}(t) = Q_0(t) + E_0(t) = Q_0(t) + 1$. The equations of motion of $E_m(t)$ are obtained from Eqs. (7)–(8) by summing these equations for $k > m$:

$$\frac{dE_m(t)}{dt} = E_{m-1}(t) + E_{m+1}(t) - (2 + \lambda m) E_m(t). \quad (9)$$

Taking into account the boundary values, we see that equation (9) is valid for all $m \geq 0$. The interpretation of the evolution equation (9) is simple: the gain terms arise from diffusion; the loss term describes diffusion and attachment (the latter occurs with rate λ onto any of the m sites of the empty interval). For a more detailed derivation of equations (7)–(9) see Ref. [12] and chapter 7 of Ref. [15].

A. Steady state weights and velocity

In the stationary state, the values of the E_m 's must satisfy the following recursion:

$$E_{m-1} + E_{m+1} = (2 + \lambda m) E_m. \quad (10)$$

We emphasize again that the boundary case $m = 0$ also fits into the pattern and therefore we have $E_1 + E_{-1} = 2$. Equation (10) is essentially the difference analog of an Airy equation. The solution of this difference equation that satisfies the boundary condition $E_0 = 1$ can be expressed in terms of Bessel functions. This can be done by comparing (10) with the well-known identity [16]

$$J_{\nu+1}(x) + J_{\nu-1}(x) = \frac{2\nu}{x} J_{\nu}(x) \quad (11)$$

for the Bessel functions. We notice that Eq. (10) is solved for all values of m (including $m = 0$) by choosing

$$E_m = \frac{J_{m+\Lambda}(\Lambda)}{J_{\Lambda}(\Lambda)} \quad \text{with} \quad \Lambda = \frac{2}{\lambda}. \quad (12)$$

Having computed these steady state probabilities, we derive the velocity of the polymer

$$v = Q_1 = 1 - E_1 = 1 - \frac{J_{\Lambda+1}(\Lambda)}{J_{\Lambda}(\Lambda)}. \quad (13)$$

This result agrees with that found in Ref. [12]. The expression (13) is compact but fairly complicated as the adsorption rate also enters into the index of the Bessel function. The plot of $v = v(\lambda)$, see figure 2, shows that in accord with intuition, the velocity is a monotonously increasing function of the adsorption rate.

To better appreciate the behavior of the velocity, let us consider the limits of small and large adsorption rate. The small λ behavior is derived from an asymptotic formula [17]

$$J_X(X+x) = \left(\frac{2}{X}\right)^{1/3} \text{Ai}(0) - \left(\frac{2}{X}\right)^{2/3} \text{Ai}'(0)x + \dots \quad (14)$$

which is valid for $X \rightarrow \infty$ and for a fixed value of x . We thus obtain

$$v = -\frac{\text{Ai}'(0)}{\text{Ai}(0)} \lambda^{1/3}. \quad (15)$$

Using the well-known expressions [16]

$$\text{Ai}(0) = \frac{1}{3^{2/3}\Gamma(2/3)}, \quad \text{Ai}'(0) = -\frac{1}{3^{1/3}\Gamma(1/3)}, \quad (16)$$

equation (15) can be rewritten as

$$v = \mathcal{A}\lambda^{1/3} \quad \text{with} \quad \mathcal{A} = \frac{3^{1/3}\Gamma(2/3)}{\Gamma(1/3)} = 0.72901113\dots \quad (17)$$

The dependence of v on λ agrees with the scaling argument given in Eq. (4). This behavior can be understood more physically as follows. Let τ be the typical time between two successive adsorptions on the leftmost empty segment. The tip will move a distance $d \sim \sqrt{\tau}$. Now we note that $\lambda d\tau \sim 1$ since λ is the adsorption rate per site. These relations imply that $\tau \sim \lambda^{-2/3}$ and $d \sim \lambda^{-1/3}$. Therefore

$$v \sim \frac{d}{\tau} \sim \lambda^{1/3}$$

explaining the $\lambda^{1/3}$ scaling. Higher orders of the expansion of the velocity with respect to the attachment rate λ can be derived from the asymptotic expansion

$$J_X(X+x) = \frac{1}{3\pi} \sum_{m \geq 0} B_m(x) \sin\left(\frac{m+1}{3}\pi\right) \Gamma\left(\frac{m+1}{3}\right) \left(\frac{X+x}{6}\right)^{-\frac{m+1}{3}} \quad (18)$$

extending the expansion of Eq. (14). (A proof of (18) can be found in the treatise [17] which also contains explicit expressions for $B_m(x)$, polynomials in x of order m , for small orders [18].) From Eq. (18) we deduce that

$$v = \mathcal{A}\lambda^{1/3} - \frac{\lambda}{10} + \frac{\mathcal{A}^2}{140} \lambda^{5/3} + \mathcal{O}(\lambda^2), \quad (19)$$

with \mathcal{A} defined in Eq. (17). This expression is more precise than (17) and it can be used for data fitting (see figure 2).

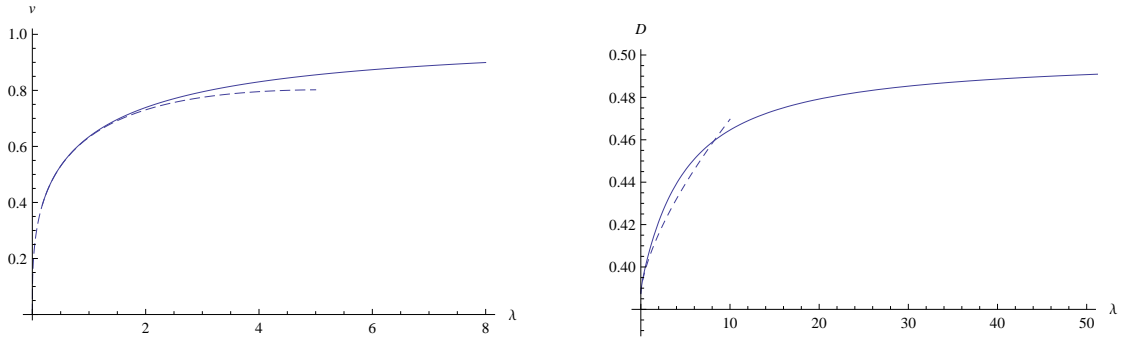


FIG. 2: Velocity and diffusion constant versus the attachment rate. The left figure displays the exact formula (13) for the velocity, the dashed line represents the asymptotic formula (19). The right figure shows the diffusion constant (31); the small λ expansion (dashed line) given by Eq. (32) is also plotted for comparison.

B. Diffusion constant and higher cumulants

The calculation of the velocity described in subsection II A relies on the steady-state probability distributions. The diffusion constant, however, cannot be determined from the steady-state distributions. Indeed, dispersion embodies information about transient states — it can be expressed in terms of integrals of two-time correlation functions [19], while the knowledge of the steady-state characteristics is insufficient. Therefore in many interacting stochastic processes the analytical determination of the diffusion constant is quite involved [19–21]. In this subsection we describe an approach that leads to an analytical expression for the diffusion constant \mathcal{D} . This approach will also allow us to compute the large deviation function which, in addition to velocity and diffusion constant, contains the entire statistics of the translocated length.

Before embarking into calculations we notice that in Ref. [12], the diffusion constant has been probed through Monte-Carlo simulations. The value $\mathcal{D} \approx 0.388$ was found numerically in the limit of vanishing deposition rate $\lambda \ll 1$, whereas in the $\lambda \rightarrow \infty$ limit the model becomes equivalent to the one-dimensional burnt-bridge model [22], for which the dispersion has been calculated in [23]. We now show how to compute $\mathcal{D}(\lambda)$ analytically.

As explained in Section I, we are interested in the statistical properties of the translocated length L in the long time limit, see (2). Since the motion of the polymer is affected only by the leftmost chaperone molecule, let us disregard the positions of other chaperone molecules and focus on $P_j(L, t)$, the probability that at time t the polymer has translocated a length L inside the cell and that the leftmost chaperone is at distance j from the pore. The evolution equations for $P_j(L, t)$ read

$$\frac{dP_j(L)}{dt} = P_{j-1}(L-1) + P_{j+1}(L+1) + \lambda \sum_{k>j} P_k(L) - [2 + \lambda(j-1)]P_j(L) \quad \text{for } j > 1, \quad (20)$$

$$\frac{dP_1(L)}{dt} = P_2(L+1) + \lambda \sum_{k>1} P_k(L) - P_1(L). \quad (21)$$

These equations are just a more comprehensive version of Eqs. (7)–(8). Using the sum rule $\sum_{L \geq j} P_j(L, t) = Q_j(t)$ which follows from the definitions of $P_j(L, t)$ and $Q_j(t)$ one can recover Eqs. (7)–(8) from Eqs. (20)–(21).

We now introduce the generating function (which is essentially the discrete Laplace transform)

$$\Pi_j(\mu, t) = \sum_L e^{\mu L} P_j(L, t) \quad (22)$$

In equations (20)–(21) and hereinafter we usually suppress the dependence on time, e.g. we shortly write $P_j(L)$ instead of $P_j(L, t)$. In addition to suppressing time dependence, we shall often suppress the dependence on the fugacity parameter μ ; for instance, Π_j means $\Pi_j(\mu, t)$.

From Eqs. (20)–(21) we deduce the governing equations for Π_j 's:

$$\frac{d\Pi_j}{dt} = e^\mu \Pi_{j-1} + e^{-\mu} \Pi_{j+1} + \lambda \sum_{k>j} \Pi_k - [2 + \lambda(j-1)] \Pi_j \quad \text{for } j > 1, \quad (23)$$

$$\frac{d\Pi_1}{dt} = e^{-\mu} \Pi_2 + \lambda \sum_{k>1} \Pi_k - \Pi_1. \quad (24)$$

Note that these equations are the same as Eqs. (7) and (8) satisfied by the Q_j 's, except for the $\exp(\pm\mu)$ factors. The infinite system of equations (23)–(24) can be rewritten in a matrix form

$$\frac{d\mathbf{\Pi}(\mu)}{dt} = \mathbb{M}(\mu)\mathbf{\Pi}(\mu). \quad (25)$$

Here $\mathbf{\Pi}(\mu)$ is a column vector $\mathbf{\Pi}(\mu) = (\Pi_1, \Pi_2, \dots)^T$ and $\mathbb{M}(\mu)$ is a matrix

$$\mathbb{M}(\mu) = \begin{pmatrix} -1 & e^{-\mu} + \lambda & \lambda & \lambda & \lambda & \lambda & \dots \\ e^\mu & -(2 + \lambda) & e^{-\mu} + \lambda & \lambda & \lambda & \lambda & \dots \\ 0 & e^\mu & -(2 + 2\lambda) & e^{-\mu} + \lambda & \lambda & \lambda & \dots \\ & 0 & e^\mu & -(2 + 3\lambda) & e^{-\mu} + \lambda & \lambda & \dots \\ & & \ddots & \ddots & & \ddots & \ddots \end{pmatrix} \quad (26)$$

For $\mu = 0$, the matrix $\mathbb{M}(0)$ is the continuous-time Markov matrix that governs the evolution of the Q_j 's. For non-vanishing μ , we can write

$$\langle e^{\mu L} \rangle = \sum_j \Pi_j(\mu, t) \sim e^{U(\mu)t} \quad \text{for } t \rightarrow \infty \quad (27)$$

with $U(\mu)$ being the largest eigenvalue of matrix $\mathbb{M}(\mu)$. (The existence and the uniqueness of the maximal eigenvalue is guaranteed by the Perron-Frobenius theorem [24].) In the long time-limit, the function $U(\mu)$ generates all the cumulants of L . Indeed, taking the logarithm of Eq. (27), and expanding it with respect to μ , one obtains

$$U(\mu) = \mu \frac{\langle L \rangle}{t} + \mu^2 \frac{\langle L^2 \rangle - \langle L \rangle^2}{2t} + \dots = \mu v + \mu^2 \mathcal{D} + \dots \quad (28)$$

Hence, $U(\mu)$ contains the full information for the long-time statistics of the translocation length; in particular, the second-order term in the Taylor expansion provides the diffusion constant.

An implicit formula for $U(\mu)$ can be derived following a path very similar to that used in the previous section to calculate the velocity v . The computations are more cumbersome [see Appendix A] but straightforward. We obtain

$$U(\mu) = (e^\mu - 1) \left(1 - \frac{J_{\Lambda[1+U(\mu)/2]+1}(\Lambda)}{J_{\Lambda[1+U(\mu)/2]}(\Lambda)} \right) \quad \text{with } \Lambda = \frac{2}{\lambda}. \quad (29)$$

A perturbative expansion for small μ allows us to calculate the cumulants of the translocated length L . At the first order we have:

$$U(\mu) = \mu \left(1 - \frac{J_{\Lambda+1}(\Lambda)}{J_{\Lambda}(\Lambda)} \right) + \mathcal{O}(\mu^2), \quad (30)$$

which agrees with the already-known expression (13) for the translocation velocity. Developing to the second order allows us to derive a formula for the diffusion constant of the polymer chain

$$\mathcal{D} = \frac{v}{2} - \frac{v}{\lambda} \left(\frac{\partial}{\partial \Lambda} \frac{J_{\Lambda+1}(x)}{J_{\Lambda}(x)} \right) \Big|_{x=\Lambda}. \quad (31)$$

We emphasize that the derivative is with respect to the order Λ of the Bessel function and not with respect to its argument x , i.e. the value $x = \Lambda$ is to be substituted after the derivative has been taken. Using the asymptotic expansion (18), we deduce

$$\mathcal{D} = \mathcal{A}^3 + \frac{\mathcal{A}^2}{30} \lambda^{2/3} + \mathcal{O}(\lambda^{4/3}) \quad (32)$$

with \mathcal{A} defined by Eq. (17). The exact formula (31) and the small λ expansion are represented in figure 2. In the leading order, we find

$$\mathcal{D} \simeq \mathcal{A}^3 = 3 \left(\frac{\Gamma(2/3)}{\Gamma(1/3)} \right)^3 = 0.3874382381 \dots \quad (33)$$

The Monte-Carlo simulation results [12] are in excellent agreement with this analytical prediction. At first sight, the agreement even seems too good: Equation (32) shows that the corrections to the limiting value are of the order $\lambda^{2/3}$, so they could be significant even for small values of the attachment rate λ . However, the amplitude in front of the correction term is very small (numerically 0.00851). This explains why in numerical simulations [12] the dispersion looks almost constant for $\lambda < 1$.

Thus we have obtained the complete statistics of the translocated length of the polymer in the situation when the chaperone molecules have the same length as the monomer units. Our chief result, Eq. (29), is an implicit highly transcendental relation for $U(\mu)$, the largest eigenvalue of matrix $\mathbb{M}(\mu)$. The generating function $U(\mu)$ is related by Legendre Transform to the large deviation function of the translocated length L (see e.g. Ref. [25] on large deviation techniques). We emphasize again that this generating function contains *all* cumulants: expanding this function, $U(\mu) = \sum_{n \geq 1} \mu^n \frac{U_n}{n!}$, we extract $v = U_1$, $\mathcal{D} = 2U_2$, see (30), and subsequent cumulants

$$U_3 = \lim_{t \rightarrow \infty} \frac{\langle L^3 \rangle - 3\langle L \rangle \langle L^2 \rangle + 2\langle L \rangle^3}{t},$$

$$U_4 = \lim_{t \rightarrow \infty} \frac{\langle L^4 \rangle - 4\langle L \rangle \langle L^3 \rangle - 3\langle L^2 \rangle^2 + 6\langle L \rangle^2 \langle L^2 \rangle}{t}, \text{ etc.}$$

Finally we note that all results of this section can be generalized to the situation when the bare polymer undergoes a biased diffusion; an outline of the computations and the final formulas for the velocity and the diffusion constant are presented in Appendix B.

III. THE CONTINUOUS SPACE MODEL

A class of proteins responsible for the translocation mechanism across the endoplasmic reticulum is known as the Hsp-70 family. Typical chaperones belonging to that family are of 2nm in size, representing roughly 6 or 7 lattice sites of the translocating polymer. The size ℓ of the chaperones can have an important quantitative effect on the translocation process, because it modifies the velocity v and the diffusion constant \mathcal{D} , as explained in Eq. (3). For chaperones of length ℓ greater than the monomer size a , the discrete model of the previous section can in principle be solved. The resulting expressions for the velocity are not explicit, however, because a linear system of ℓ equations must be solved in order to adjust the boundary conditions [12]. Here we examine the limiting case when the length of the chaperone molecule vastly exceeds the monomer size. Keeping the chaperone of size ℓ finite we therefore consider the $a \rightarrow 0$ limit when the discrete lattice turns into a continuous line.

We set again the length ℓ of the chaperone protein and the bare diffusion constant D to unity. With this agreement, the dimensionless attachment rate $\lambda \ell^3 / D$ is equal to λ . Thus mathematically the chaperon molecules are segments of unit length that absorb onto a continuous line with rate λ . Adsorption problems where the substrate is the continuous line are usually solvable if the analogous problems where the substrate is the one-dimensional lattice are tractable [15].

Let $Q(x, t)dx$ be the probability that the left edge of the first absorbed chaperone on the right of the pore is located between x and $x + dx$, see figure 3. Further, denote by $E(x, t)$ the probability that the first chaperone molecule is more than a distance x away. The relation between these two probabilities is

$$E(x, t) = \int_x^\infty dy Q(y, t) \quad (34)$$

The probability densities $Q(x, t)$ satisfy

$$\frac{\partial Q}{\partial t} = \frac{\partial^2 Q}{\partial x^2} - \lambda(x-1)Q + \lambda \int_{x+1}^\infty dy Q(y), \quad x \geq 1 \quad (35a)$$

$$\frac{\partial Q}{\partial t} = \frac{\partial^2 Q}{\partial x^2} + \lambda \int_{x+1}^\infty dy Q(y), \quad x < 1 \quad (35b)$$

These equations can be derived directly by studying how $Q(x, t)$ varies between time t and $t + dt$. One can also obtain them as continuous limits of the discrete equations (7) and (8).

The governing equations for the empty interval probabilities $E(x, t)$ are

$$\frac{\partial E}{\partial t} = \frac{\partial^2 E}{\partial x^2} - \lambda(x-1)E - \lambda \int_x^{x+1} dy E(y), \quad x \geq 1 \quad (36a)$$

$$\frac{\partial E}{\partial t} = \frac{\partial^2 E}{\partial x^2} - \lambda \int_1^{x+1} dy E(y), \quad x < 1 \quad (36b)$$

In the large time limit, $Q(x, t)$ and $E(x, t)$ become stationary. Here we focus on the stationary empty interval probabilities $E(x) \equiv E(x, t = \infty)$ that satisfy

$$\frac{d^2 E}{dx^2} = \lambda(x-1)E(x) + \lambda \int_x^{x+1} dy E(y), \quad x \geq 1 \quad (37a)$$

$$\frac{d^2 E}{dx^2} = \lambda \int_1^{x+1} dy E(y), \quad x < 1 \quad (37b)$$

This set of integro-differential equations can be viewed as a generalization of the classical Airy equation [26]. Essentially, we need to solve (37a); the solution of (37b) will then be found by a simple integration as the right-hand side is known. Equation (37a) is non-local as can be seen by differentiating it with respect to x :

$$\frac{d^3 E(x)}{dx^3} = \lambda(x-2) \frac{dE(x)}{dx} + \lambda E(x+1)$$

In the following, we derive an exact solution of Eqs. (37a)–(37b).

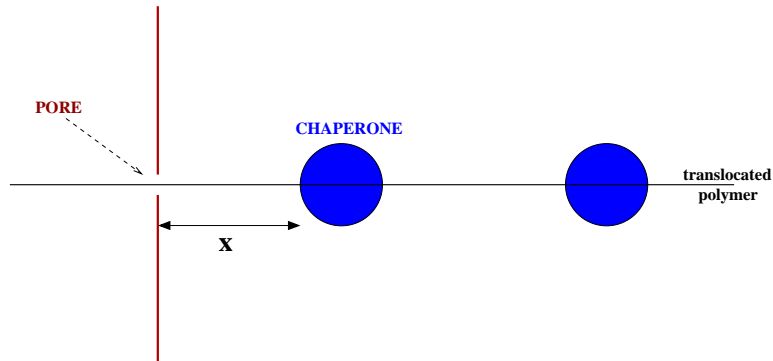


FIG. 3: Illustration of chaperone-assisted translocation for the continuous model.

A. Stationary solution and velocity

For difference-differential equations, it is difficult even to prescribe the boundary conditions; formally one needs to have a boundary condition on the interval of length 1, say $E(x)$ on interval $1 \leq x \leq 2$, and then one can construct the solution for all $x > 1$. For almost any choice of the ‘boundary values’ the resulting solution will be unacceptable (diverging at $x \rightarrow \infty$ rather than vanishing, not decreasing monotonously with x , etc...). Rather than proceeding in a formal manner, we shall use here the Laplace method (see e.g. [27] or [28]) which is a very powerful approach allowing one to deal with linear differential equations whenever coefficients are linear functions of x . This constraint is met in our case, so we employ the Laplace method. This method tells one to seek a solution in the form

$$E(x) = \int_C du e^{ux} Z(u) \quad (38)$$

where the integral is taken over a contour C in a complex plane to be specified at a later stage.

We determine $Z(u)$ by inserting (38) into the governing equation (37a). The left-hand side is

$$\frac{d^2 E}{dx^2} = \int_C du e^{ux} u^2 Z(u)$$

The non-local term on the right-hand side becomes

$$\int_x^{x+1} dy E(y) = \int_C du e^{ux} \frac{e^u - 1}{u} Z(u)$$

To simplify $x E(x)$ we use integration by parts

$$\begin{aligned} x E(x) &= \int_C du e^{ux} x Z(u) \\ &= e^{ux} Z(u)|_C - \int_C du e^{ux} \frac{dZ}{du} \\ &= - \int_C du e^{ux} \frac{dZ}{du} \end{aligned}$$

where the validity of the last result relies on the assumption that function $e^{ux} Z(u)$ has the same value on both ends of the contour C . Combining above results we find that (38) is a solution to Eq. (37a) if $Z(u)$ obeys

$$u^2 Z = -\lambda Z - \lambda \frac{dZ}{du} + \lambda \frac{e^u - 1}{u} Z$$

Solving this differential equation we find

$$Z = \text{const} \cdot \exp\left(-u - \frac{u^3}{3\lambda} + \int_0^u dv \frac{e^v - 1}{v}\right) \quad (39)$$

If we take the contour C that goes from infinity to the origin along the ray with $\arg(u) = \frac{3\pi}{2} - \epsilon$ and then goes back to infinity along the ray with $\arg(u) = \frac{\pi}{2} + \epsilon$ (see figure 4), then $e^{ux} Z(u)$ vanishes on both ends of the contour C (as long as $0 < \epsilon < \pi/6$). In the $\epsilon \rightarrow +0$ limit, the contour C coincides with the imaginary axis. Writing $u = iw$ we obtain the desired integral representation

$$E(x) = A \int_0^\infty dw C(w) C(w, x) \quad (40)$$

with

$$\begin{aligned} C(w) &= \exp\left(\int_0^w dv \frac{\cos v - 1}{v}\right) \\ C(w, x) &= \cos[w(x-1) + W] \\ W = W(w) &= \frac{w^3}{3\lambda} + \int_0^w dv \frac{\sin v}{v} \end{aligned} \quad (41)$$

and yet undetermined constant A . Equation (40) is valid for $x \geq 1$ and can be used to determine the behavior of $E(x)$ at large x (see Appendix C 1).

The above solution (38)–(39) is valid for $x > 1$. Using these results we reduce equation (37b) governing the small size ($x < 1$) behavior to

$$\frac{d^2 E}{dx^2} = \lambda A \int_0^\infty dw C(w) \frac{\sin(wx + W) - \sin(W)}{w}. \quad (42)$$

Integrating (42) subject to $E(0) = 1$ we obtain

$$E = 1 - Bx - \lambda A \int_0^\infty dw C(w) \Phi(w, x) \quad (43)$$

$$\text{with } \Phi = \frac{\sin(wx + W) - \sin W - wx \cos W}{w^3} + x^2 \frac{\sin W}{2w}. \quad (44)$$

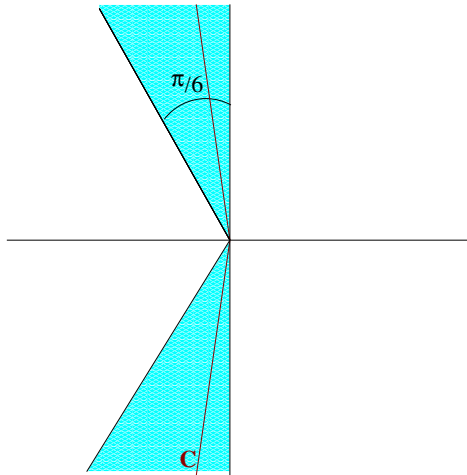


FIG. 4: Contour in the complex plane which has been used in the implementation of Laplace's method in Eq. (38). The shaded domain (with opening angle equal to $\pi/6$) shows the region in which the contour C can exist and leads to a well defined function $Z(u)$.

The constants A and B are determined using the fact that the probability $E(x)$ is continuous, and therefore the two expressions, (40) and (43), must match at $x = 1$. This gives

$$\frac{1-B}{A} = \int_0^\infty dw \mathcal{W}_1(w) C(w) \quad (45)$$

$$\text{with } \mathcal{W}_1 = \cos W + \lambda \frac{\sin(w+W) - (1 - \frac{w^2}{2}) \sin W - w \cos W}{w^3} \quad (46)$$

We should further equate the derivatives of $E(x)$ at the matching point. This yields

$$\frac{B}{A} = \int_0^\infty dw \mathcal{W}_2(w) C(w) \quad (47)$$

$$\text{with } \mathcal{W}_2 = w \sin W - \lambda \frac{\cos(w+W) - \cos W + w \sin W}{w^2}. \quad (48)$$

Equation (40) and Eqs. (43)–(48) determine the probabilities $E(x)$ in the stationary regime. The knowledge of these stationary empty interval probabilities allows us to compute the velocity. Using $v = -E'(0)$, we deduce from (43) that $v = B$. [The relation $v = -E'(0)$ is the continuous version of (13).] Equations (45)–(47) in conjunction with $v = B$ lead to the following expression for the velocity:

$$v = \frac{\int_0^\infty dw \mathcal{W}_2(w) C(w)}{\int_0^\infty dw [\mathcal{W}_1(w) + \mathcal{W}_2(w)] C(w)}. \quad (49)$$

This formula can be used to plot v as a function of the attachment rate λ , see figure 5, and to extract asymptotic expansions. In the case $\lambda \rightarrow 0$, we make the change of variable $w = \lambda^{1/3} \omega$ in Eq. (49). Taking the $\lambda \rightarrow 0$ limit and keeping ω finite, we find that the dominant behaviors of the expressions in Eqs. (41), (46) and (48) are given by

$$C = 1, \quad W = \frac{\omega^3}{3}, \quad \mathcal{W}_1 = \cos\left(\frac{\omega^3}{3}\right) \quad \text{and} \quad \mathcal{W}_2 = \lambda^{1/3} \omega \sin\left(\frac{\omega^3}{3}\right). \quad (50)$$

Substituting in Eq. (49), we obtain the leading behavior of the speed

$$v = \lambda^{1/3} \frac{\int_0^\infty d\omega \omega \sin\left(\frac{\omega^3}{3}\right)}{\int_0^\infty d\omega \cos\left(\frac{\omega^3}{3}\right)} = \frac{3^{1/3} \Gamma(2/3)}{\Gamma(1/3)} \lambda^{1/3}. \quad (51)$$

This result agrees with the prediction for the discrete model, Eq. (17). This agreement is not surprising — in the limit of infinitely small attachment rate, the discreteness of the polymer does not play any role and the system behaves as if it were effectively continuous.

The $\lambda \rightarrow \infty$ limit is more difficult to implement (see Appendix D), yet the final result is remarkably simple

$$v \rightarrow 2 \quad \text{when} \quad \lambda \rightarrow \infty. \quad (52)$$

We can understand (52) as follows. In the $\lambda \rightarrow \infty$ limit, a chaperone is attached as soon as the translocated segment length reaches 1. The model becomes equivalent to a continuous time random walker on a discrete lattice, that can only make forward steps of unit length. The randomness in the problem arises from the distribution $\psi(T)$ of the waiting time T between two successive jumps. The distribution $\psi(T)$ is identical to that of the first passage time at $x = 1$ of a Brownian motion starting at $x = 0$ with a reflecting boundary at $x = 0$ and an absorbing boundary at $x = 1$. The Laplace transform $\hat{\psi}(p) = \langle e^{pT} \rangle$ is obtained by utilizing standard techniques [15, 29, 30] to yield

$$\hat{\psi}(p) = \frac{1}{\cosh \sqrt{p}}. \quad (53)$$

The velocity is then found to be

$$v = \frac{1}{\langle T \rangle} = -\frac{1}{\hat{\psi}'(0)} = 2.$$

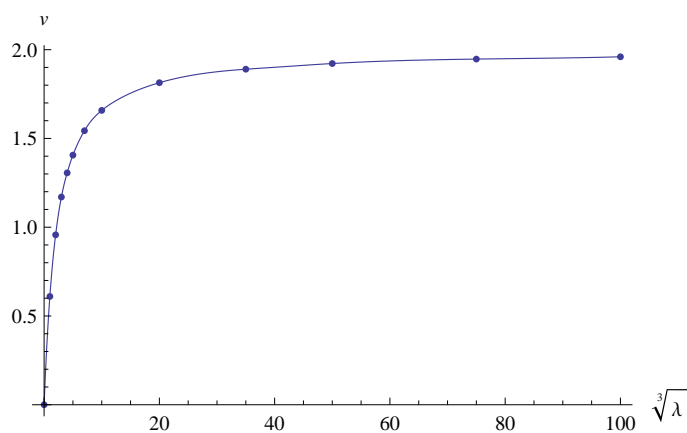


FIG. 5: Plot of the velocity v of the continuous model as a function of $\lambda^{1/3}$ using the exact formula (49). The integrals that appear in the numerator and denominator of expression (49) were evaluated for various values of λ ranging between 1 and 10^6 (represented as dots in the figure) and a smooth interpolating curve was drawn to join these points. We observe that for large values of λ , we have $v \rightarrow 2$. An empirical approximation, valid for $\lambda^{1/3} \geq 10$, is given by $v = 2 - \frac{c_1}{\lambda^{1/3}} + \frac{c_2}{\lambda^{2/3}} \dots$ with $c_1 \simeq 4$ and $c_2 \simeq 6$.

B. Calculation of the diffusion constant

The diffusion constant \mathcal{D} of the continuous translocation model can be derived by utilizing the same approach as in the discrete case. Namely, we shall establish an implicit equation for the large deviation function $U(\mu)$. Mathematically, one has to find the largest eigenvalue of a suitable differential operator \mathcal{L}_μ which is a deformation (with respect to the parameter μ) of the evolution operator for E that appears in Eqs. (D5). One also has to be careful of how the boundary conditions are deformed.

The details of the calculations are given in Appendix D and the solution for $U(\mu)$ is presented in Eq. (D15). Having computed $U(\mu)$, we can retrieve the formula (49) for the velocity (by expanding $U(\mu)$ to the first order with respect to μ). The coefficient of the μ^2 term gives the diffusion constant \mathcal{D} . The calculations are rather involved but systematic. The explicit expression for \mathcal{D} is given in Eqs. (D16) to (D17). Although the results look unwieldy, they can be used to derive asymptotic limits for very small or very large values of the attachment rate λ .

In the case $\lambda \rightarrow 0$ we make again the change of variable $w = \lambda^{1/3}\omega$. Using (50)–(51) we find the leading behavior of the functions $\delta C, \delta \mathcal{W}_1, \delta \mathcal{W}_2$ (see Appendix D for definitions)

$$\delta C = -\frac{\omega^2}{\lambda^{1/3}}, \quad \delta \mathcal{W}_1 = -\frac{\mathcal{A}}{\lambda^{1/3}} \omega \sin\left(\frac{\omega^3}{3}\right), \quad \delta \mathcal{W}_2 = \mathcal{A} \omega^2 \cos\left(\frac{\omega^3}{3}\right). \quad (54)$$

From this information we extract the limiting behavior of \mathcal{D} by analyzing each contribution in Eq. (D16):

$$\mathcal{D} \simeq 1 - v \frac{\int_0^\infty dw C \delta \mathcal{W}_1}{\int_0^\infty dw [\mathcal{W}_1 + \mathcal{W}_2] C} + \frac{\int_0^\infty dw \mathcal{W}_2 \delta C}{\int_0^\infty dw [\mathcal{W}_1 + \mathcal{W}_2] C} + o(1) \quad (55)$$

Substituting the dominant behaviors found above, (50)–(51) and (54), we arrive at

$$\mathcal{D} \simeq 1 + \mathcal{A}^2 \frac{\int_0^\infty d\omega \omega \sin \frac{\omega^3}{3}}{\int_0^\infty d\omega \cos \frac{\omega^3}{3}} - \frac{\int_0^\infty d\omega \omega^3 \sin \frac{\omega^3}{3}}{\int_0^\infty d\omega \cos \frac{\omega^3}{3}}. \quad (56)$$

Calculating the integrals in the above formula (the numerator in the third term is determined using analytic continuation and we find that the third term is equal to -1), we obtain, in agreement with the result of Eq. (33) for the discrete case,

$$\mathcal{D} \simeq \mathcal{A}^3 \quad \text{when} \quad \lambda \rightarrow 0. \quad (57)$$

The case $\lambda \rightarrow \infty$ is analyzed using techniques and tricks similar to those involved for deriving the large λ asymptotics in the discrete case (see Appendix D for details). A precise investigation of the asymptotic behavior of each of the terms that appear in the formula (D16) for the diffusion constant can be carried out. The calculations are systematic and in principle straightforward, but very lengthy; the final result is shockingly compact

$$\mathcal{D} \rightarrow \frac{2}{3} \quad \text{when} \quad \lambda \rightarrow \infty. \quad (58)$$

This value is in perfect agreement with the one obtained for the continuous time random walker model with waiting time T distributed according to the law $\psi(T)$ with Laplace transform $\hat{\psi}(p)$ given in Eq. (53). For this effective problem, the diffusion constant is found to be

$$\mathcal{D} = \frac{1}{2} \frac{\langle T^2 \rangle - \langle T \rangle^2}{\langle T \rangle^3} = \frac{1}{2} \frac{\hat{\psi}''(0) - [\hat{\psi}'(0)]^2}{[-\hat{\psi}'(0)]^3} = \frac{2}{3}.$$

We remark that for very large values of the attachment rate λ , the chaperon-assisted translocation model becomes equivalent to the burnt bridge model with periodic bridges [23]. The velocity and diffusion coefficient for this model are known and using these results it is possible to determine the velocity and the diffusion coefficient for the chaperon-assisted translocation in the $\lambda \rightarrow \infty$ limit. The connection with the burnt bridge model with periodic bridges holds even in the general discrete case with arbitrary ℓ/a [12]; if $\ell/a \rightarrow \infty$, the limiting values $v = 2$ and $\mathcal{D} = 2/3$ are recovered. Finally we note that the generating function technique employed in this study can be adapted to a calculation of the large deviation function of the burnt bridge model.

IV. DISCUSSION

The mechanism that drives the translocation of a protein through a membrane depends on chemical asymmetries between the cis and trans sides of the membrane [4]. There can be several mechanisms leading to asymmetry and they can be simultaneously present. In this work, we have studied a model where asymmetry arises due to the preferential binding of proteins on the translocated segment of the polymer. The mathematical effect that gives raise to directed motion is the Brownian ratchet model that plays a crucial role in the field of molecular motors [31–34]. It is important to note that the ratchet paradigm is quite insensitive to the precise mechanism at the molecular level. The key ingredients are the breaking of spatial symmetry and a supply of free energy which insures here a sufficiently strong binding of the chaperone on the polymer. In biological context, the free energy source is usually provided by ATP hydrolysis [6, 35].

From the point of view of statistical physics, it is interesting to note that these models, which are effectively one-dimensional, can be mapped to variants of driven diffusive gases and can be studied through techniques which were developed to understand the physics of non-equilibrium systems. These methods not only reveal underlying time-reversal symmetries of the system, but also provide powerful computational tools. For example, the technique based on the deformation of the master operator can be traced back to the proof of the Gallavotti-Cohen fluctuation theorem for Langevin dynamics and for Markov processes by Kurchan [36] and by Lebowitz and Spohn [37]. In the present work, we have assumed that the attachment of chaperones is irreversible; if the detachment rate were positive, the fluctuation theorem would be valid. The analysis carried out in this paper heavily relies on the fact that the

equations of motion depend only on the position of the chaperone closest to the pore. If the chaperones could detach from the polymer, the above property would no longer be true and the positions of all the chaperones bound at a given time to the polymer must be taken into account. The system would turn into an M -body problem with both M (the number of currently attached chaperon molecules) and L (the current length of the translocated polymer) being random variables. This appears to be a very challenging unsolved model. Besides, similar descriptions appear in mass transport models within a fungal hypha with mutually excluding particles progressing in a stochastic manner along a growing one-dimensional lattice [38].

Acknowledgments

We are grateful to Tibor Antal, Sid Redner and Shamlal Mallick for useful discussions and careful reading of the manuscript. PLK thanks NSF grant CCF-0829541 for support.

Appendix A: Calculation of the Cumulant Generating Function

In this Appendix, we show that the maximal eigenvalue $U(\mu)$ of matrix $\mathbb{M}(\mu)$, defined in Eq. (26), is indeed given by Eq. (29).

Let G_1, G_2, \dots be the components of the eigenvector corresponding to the maximal eigenvalue $U(\mu)$. The eigenvalue equation reads

$$U(\mu)G_j = e^\mu G_{j-1} + e^{-\mu} G_{j+1} + \lambda \sum_{k>j} G_k - [2 + \lambda(j-1)] G_j \quad \text{for } j > 1, \quad (\text{A1})$$

$$U(\mu)G_1 = e^{-\mu} G_2 + \lambda \sum_{k>1} G_k - G_1 = e^\mu G_0 + e^{-\mu} G_2 + \lambda \sum_{k>1} G_k - 2G_1, \quad (\text{A2})$$

where, in order to fit the equation for $j = 1$ into the general pattern, we have defined $e^\mu G_0 = G_1$. As in the beginning of Section II, it is useful to introduce $\Gamma_m = \sum_{k>m} G_k$, defined for $m \geq -1$. Then, for all $m \geq 0$, the following equation is satisfied:

$$U(\mu)\Gamma_m = e^{-\mu}\Gamma_{m+1} - (2 + \lambda m)\Gamma_m + e^\mu\Gamma_{m-1}. \quad (\text{A3})$$

The value of Γ_0 is fixed by imposing the normalization constraint: $\Gamma_0 = 1$. (This overall proportionality constant does not affect the final result.) Equation (A3) for $m = 0$ then gives

$$e^{-\mu}\Gamma_1 + e^\mu\Gamma_{-1} = 2 + U(\mu). \quad (\text{A4})$$

In terms of the Γ 's, the boundary condition $e^\mu G_0 = G_1$ becomes

$$\Gamma_{-1} + \Gamma_1 e^{-\mu} = 1 + e^{-\mu}. \quad (\text{A5})$$

To solve Eq. (A3) with the boundary conditions (A4) and (A5), we use the following ansatz:

$$\Gamma_m = \frac{J_{m+r}(x)}{J_r(x)} e^{m\mu}, \quad (\text{A6})$$

where r and x have to be determined. Combining Eqs. (A3) and (A6), we get

$$x = 2/\lambda = \Lambda \quad \text{and} \quad r\lambda = 2 + U(\mu). \quad (\text{A7})$$

Hence

$$\Gamma_m = \frac{J_{m+r}(\Lambda)}{J_r(\Lambda)} e^{m\mu}. \quad (\text{A8})$$

The normalization $\Gamma_0 = 1$ is satisfied. We eliminate Γ_{-1} between Eqs. (A4) and (A5) and obtain

$$\Gamma_1(1 - e^{-\mu}) = e^\mu - 1 - U(\mu) = e^\mu + 1 - r\lambda. \quad (\text{A9})$$

Taking Γ_1 from (A8) and inserting it into (A9) we obtain

$$r\lambda + (e^\mu - 1) \frac{J_{r+1}(\Lambda)}{J_r(\Lambda)} = e^\mu + 1. \quad (\text{A10})$$

Using $U = r\lambda - 2$ and extracting $r\lambda$ from (A10) we arrive at the announced implicit equation (29) for $U(\mu)$.

Appendix B: The case of a driven polymer

Here we generalize the analysis of Section II to the case of an asymmetric motion of the translocating polymer. We suppose that the polymer is driven by a non-zero force F through the pore: this can be modeled by saying that the polymer hops to the right with rate p and to the left with rate q with $p/q = e^F$. The basic equations now become

$$\frac{dQ_j}{dt} = pQ_{j-1} + qQ_{j+1} + \lambda \sum_{k>j} Q_k - [p + q + \lambda(j-1)] Q_j \quad \text{for } j > 1, \quad (\text{B1})$$

$$\frac{dQ_1}{dt} = qQ_2 + \lambda \sum_{k>1} Q_k - pQ_1. \quad (\text{B2})$$

One has to define Q_0 such that $pQ_0 = qQ_1$.

In the stationary state, the equations for the E_m 's defined as $E_m = \sum_{k>m} Q_k$ become

$$pE_{m-1} + qE_{m+1} = (p + q + \lambda m) E_m, \quad (\text{B3})$$

with $E_0 = 1$ and $pE_{-1} + qE_1 = p + q$. The solution of this difference equation that satisfies the boundary condition is

$$E_m = \left(\frac{p}{q}\right)^{m/2} \frac{J_{m+\Lambda}(\bar{\Lambda})}{J_{\Lambda}(\bar{\Lambda})} \quad \text{with } \Lambda = \frac{p+q}{\lambda} \quad \text{and } \bar{\Lambda} = \frac{2\sqrt{pq}}{p+q} \Lambda. \quad (\text{B4})$$

This leads us to the velocity of the polymer:

$$v = p + q(Q_1 - 1) = p - qE_1 = p - \sqrt{pq} \frac{J_{\Lambda+1}(\bar{\Lambda})}{J_{\Lambda}(\bar{\Lambda})}, \quad (\text{B5})$$

Similarly, we derive the following equation for the maximal eigenvalue and the corresponding eigenvector for the cumulant generating deformed matrix:

$$pe^{\mu}\Gamma_{m-1} + qe^{-\mu}\Gamma_{m+1} = (p + q + \lambda m + U(\mu)) \Gamma_m, \quad (\text{B6})$$

which is valid for $m \geq 0$ with boundary conditions $\Gamma_0 = 1$ and $p(\Gamma_{-1} - 1) + qe^{-\mu}(\Gamma_1 - 1) = 0$. This leads us to the implicit equation for $U(\mu)$:

$$U(\mu) = (e^{\mu} - 1) \left(p - \sqrt{pq} \frac{J_{\Lambda(1+\frac{U}{p+q})+1}(\bar{\Lambda})}{J_{\Lambda(1+\frac{U}{p+q})}(\bar{\Lambda})} \right). \quad (\text{B7})$$

Expanding (B7) to the first order in μ we recover velocity and an expansion to the second order gives the diffusion constant:

$$\mathcal{D} = \frac{v}{2} - \sqrt{pq} \frac{v}{\lambda} \left(\frac{\partial}{\partial \Lambda} \frac{J_{\Lambda+1}(x)}{J_{\Lambda}(x)} \right) \Big|_{x=\bar{\Lambda}} \quad (\text{B8})$$

Appendix C: Asymptotic expansions for the continuous polymer model

1. Large x behavior of $E(x)$

To compute the large x asymptotic, we apply the steepest decent technique on Eqs. (38)–(39). These equations show that we need to integrate $e^{F(u)}$ along the contour in the complex u plane with

$$F(u) = u(x-1) - \frac{u^3}{3\lambda} + \int_0^u dv \frac{e^v - 1}{v} \quad (\text{C1})$$

We must find the stationary point u_* where $F'(u_*)$ vanishes and deform the contour so that it passes through the stationary point in the direction of steepest decent. Using (C1) we get

$$x - 1 - \frac{u_*^2}{\lambda} + \frac{e^{u_*} - 1}{u_*} = 0 \quad (\text{C2})$$

for the critical point and we see that the direction of the steepest decent is along the imaginary axis. When $x \gg 1$, we have

$$u_* = -\sqrt{\lambda(x-1)} - \frac{1}{2(x-1)} + \mathcal{O}(x^{-5/2}) \quad (\text{C3})$$

Writing $u = u_* + iw$ and knowing that the constant that appears in (39) is equal to $(-iA/2)$, we recast (38)–(39) into

$$E = \frac{A}{2} e^{F_*} \int_{-\infty}^{\infty} dw \exp\left(-\sqrt{\frac{x-1}{\lambda}} w^2\right) \quad (\text{C4})$$

where $F_* = F(u_*)$. Computing the Gaussian integral in (C4) and using (C3) to simplify F_* we deduce

$$E = A \frac{e^{\gamma_E \sqrt{\pi}}}{2} \lambda^{3/4} (x-1)^{1/4} \exp\left[-\frac{2}{3} \sqrt{\lambda} (x-1)^{3/2}\right]$$

where $\gamma_E = 0.5772\dots$ is the Euler's constant.

2. Large λ behavior of the velocity

We calculate the leading behavior of the velocity in the $\lambda \rightarrow \infty$ limit by studying separately the numerator and the denominator in Eq. (49). Keeping only the dominant terms in λ , we find, using Eqs. (46)–(48),

$$\int_0^{\infty} dw \mathcal{W}_1(w) C(w) \simeq \lambda \int_0^{\infty} dw \frac{C(w)}{w^3} \left(\sin(w+W) - \left(1 - \frac{w^2}{2}\right) \sin W - w \cos W \right) + \mathcal{O}(1), \quad (\text{C5})$$

$$\int_0^{\infty} dw \mathcal{W}_2(w) C(w) \simeq -\lambda \int_0^{\infty} dw \frac{C(w)}{w^2} (\cos(w+W) - \cos W + w \sin W) + \mathcal{O}(1). \quad (\text{C6})$$

The function $W(w)$, see (41), is given by

$$W(w) = \int_0^w dv \frac{\sin v}{v} + \frac{w^3}{3\lambda} \equiv W_0(w) + \frac{w^3}{3\lambda},$$

where we have denoted by $W_0(w)$ the leading behavior. One could expect that the dominant behavior can be found by substituting W_0 in place of W in the expressions (C5) and (C6). But in fact, we have

$$\int_0^{\infty} dw \frac{C(w)}{w^3} \left(\sin(w+W_0) - \left(1 - \frac{w^2}{2}\right) \sin W_0 - w \cos W_0 \right) = 0, \quad (\text{C7})$$

$$\int_0^{\infty} dw \frac{C(w)}{w^2} \left(\cos(w+W_0) - \cos W_0 + w \sin W_0 \right) = 0. \quad (\text{C8})$$

We now explain why these integrals vanish identically. Because the integrands are even functions of w (recall that $C(w)$ is even and $W_0(w)$ is odd), we can replace the lower bound 0 in both the integrals by $-\infty$.

Before deriving (C7)–(C8), we shall prove a much simpler identity. Let us show that the following relation is satisfied:

$$\int_0^{\infty} dw C(w) \cos(w+W_0) = \frac{1}{2} \int_{-\infty}^{\infty} dw C(w) \cos(w+W_0) = 0. \quad (\text{C9})$$

We can add to this expression the following integral which vanishes because the integrand is odd

$$\frac{i}{2} \int_{-\infty}^{\infty} dw C(w) \sin(w+W_0) = 0. \quad (\text{C10})$$

Then, using the explicit expressions (41) for $C(w)$ and $W_0(w)$, and defining the function

$$\mathcal{E}(w) = \int_0^w dv \frac{e^{iv} - 1}{v}, \quad (\text{C11})$$

the identity (C9) becomes equivalent to

$$\int_{-\infty}^{\infty} dw C(w) e^{i(w+W_0)} = \int_{-\infty}^{\infty} dw e^{\mathcal{E}(w)} e^{iw} = 0. \quad (\text{C12})$$

This integral converges in the w -complex plane for w with positive imaginary value (i.e. $\Im(w) \geq 0$). The value of the integral will therefore be unchanged if we deform the real axis $(-\infty, +\infty)$ into any contour located in the upper half-plane. One can take for example $w = y + ib$ with $-\infty < y < \infty$ and a fixed, strictly positive, value of b . Substituting this expression for w in Eq. (C12), we observe that e^{-b} appears as a prefactor and that the rest of the integral remains bounded as b varies; taking the $b \rightarrow +\infty$ limit proves that the value of integral is indeed 0. A more elegant way to prove that the integral in Eq. (C12) vanishes identically is to deform the real axis as shown in Fig. 6.

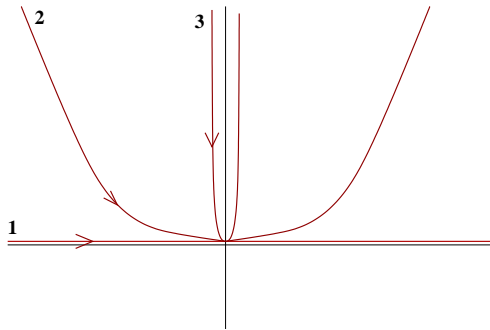


FIG. 6: Contour deformation in the upper complex plane used to prove Eqs. (C5), (C7) and (C12). The final contour follows the positive imaginary axis down from $+i\infty$ to 0 and then back from 0 to $+i\infty$. There are no singularities or cuts on the imaginary axis, therefore the two halves of the contour simply cancel with each other.

Utilizing the same approach, one can prove the following identities:

$$\int_{-\infty}^{\infty} dw e^{\mathcal{E}(w)} \frac{e^{iw} - 1}{w} = 0, \quad (\text{C13})$$

$$\int_{-\infty}^{\infty} dw e^{\mathcal{E}(w)} \frac{e^{iw} - 1 - iw}{w^2} = 0, \quad (\text{C14})$$

$$\int_{-\infty}^{\infty} dw e^{\mathcal{E}(w)} \frac{e^{iw} - 1 - iw + w^2/2}{w^3} = 0. \quad (\text{C15})$$

Note that Eq. (C8) is the real part of Eq. (C14) and Eq. (C7) is the imaginary part of Eq. (C15).

In order to find the asymptotic expression for the velocity in the large λ limit, it is thus not enough to replace W by W_0 in the expressions (C5) and (C6) and we must perform an expansion to the next order. The leading behavior of the integral $\int dw \mathcal{W}_1(w) C(w)$ is obtained by subtracting from the right-hand side of Eq. (C5) the left-hand side of Eq. (C7). There are three terms which we now analyze separately. For the first term we obtain

$$\begin{aligned} \int_0^{\infty} dw \frac{C(w)}{w^3} (\sin(w+W) - \sin(w+W_0)) &= 2 \int_0^{\infty} dw \frac{C(w)}{w^3} \sin\left(\frac{w^3}{6\lambda}\right) \cos\left(w + \frac{w^3}{6\lambda} + W_0\right) \\ &= \frac{2}{\lambda^{2/3}} \int_0^{\infty} dx \frac{C(\lambda^{1/3}x)}{x^3} \sin\frac{x^3}{6} \cos\left(\lambda^{1/3}x + \frac{x^3}{6} + W_0(\lambda^{1/3}x)\right) \end{aligned}$$

where in the second line we have made the change of variables $w \rightarrow \lambda^{1/3}x$. For large values of the argument w , we have $C(w) \simeq e^{\gamma_E}/w$ and $W_0(w) \rightarrow \pi/2$. Therefore, the above term is of order $\mathcal{O}(\lambda^{-1})$.

For the second term, we find

$$\begin{aligned} - \int_0^{\infty} dw \frac{C(w)}{w^3} \left(1 - \frac{w^2}{2}\right) (\sin(W) - \sin(W_0)) &= \int_0^{\infty} dx \frac{C(\lambda^{1/3}x)}{x^3} \left(x^2 - \frac{2}{\lambda^{2/3}}\right) \sin\frac{x^3}{6} \cos\left(\frac{x^3}{6} + W_0\right) \\ &\simeq - \frac{e^{\gamma_E}}{\lambda^{1/3}} \int_0^{\infty} dx \left(\frac{\sin x^3/6}{x}\right)^2 \end{aligned}$$

where in the last equation we have inserted the asymptotics of C and W_0 for large values of the argument and kept only the dominant term.

Finally the third term reads

$$\int_0^\infty dw \frac{C(w)}{w^2} (\cos W_0 - \cos W) = \frac{2}{\lambda^{1/3}} \int_0^\infty dx \frac{C(\lambda^{1/3}x)}{x^2} \sin \frac{x^3}{6} \sin \left(\frac{x^3}{6} + W_0(\lambda^{1/3}x) \right)$$

and it scales as $\lambda^{-2/3}$ since $C(w) \sim w^{-1}$ for large w .

Comparing these asymptotics we see that the leading contribution arises from the second term. Thus the integral (C5) is equal to

$$\int_0^\infty dw \mathcal{W}_1(w) C(w) = -\lambda^{2/3} e^{\gamma_E} \int_0^\infty dx \left(\frac{\sin x^3/6}{x} \right)^2 = -\lambda^{2/3} \frac{e^{\gamma_E} 3^{1/6} \Gamma(2/3)}{4} \quad (\text{C16})$$

in the leading order. Using a similar reasoning, we find the leading behavior of the integral (C6)

$$\int_0^\infty dw \mathcal{W}_2(w) C(w) = 2\lambda^{2/3} e^{\gamma_E} \int_0^\infty dx \left(\frac{\sin x^3/6}{x} \right)^2 \quad (\text{C17})$$

Substituting (C16)–(C17) into the formula (49) for the velocity shows that $v \rightarrow 2$ when $\lambda \rightarrow \infty$ as written in Eq. (52).

Appendix D: Generating function of the continuous polymer

In this appendix, we investigate the time evolution of the probability density $P(L, x, t)$ in the continuum setting. By definition, $P(L, x, t)dLdx$ represents the probability that the total length of the translocated polymer inside the cell is between L and $L + dL$ and that the distance of the leftmost adsorbed chaperone from the pore is between x and $x + dx$. The probability density $P(L, x, t)$ evolves according to

$$\frac{\partial P}{\partial t} = \frac{\partial^2 P}{\partial x^2} + 2 \frac{\partial^2 P}{\partial x \partial L} + \frac{\partial^2 P}{\partial L^2} - \lambda(x-1)\Theta(x-1)P + \lambda \int_{x+1}^\infty dy P(L, y, t). \quad (\text{D1})$$

The Heaviside function $\Theta(x-1)$ ensures that this equation is valid for all values of $x > 0$. If we study what happens in the vicinity of the $x = 0$ boundary, we observe that the correct boundary condition is given by

$$\frac{\partial P}{\partial x} + \frac{\partial P}{\partial L} = 0 \quad \text{for } x = 0, L \geq 0. \quad (\text{D2})$$

(This boundary condition can be obtained by writing the equation in a discrete form near $x = 0$.) It is useful to consider the Laplace transform of $P(L, x)$ with respect to L

$$\hat{P}(\mu, x, t) = \int_0^\infty dL e^{\mu L} P(L, x, t), \quad (\text{D3})$$

and to use the cumulative function

$$\mathcal{E}(\mu, x, t) = \int_x^\infty dy \hat{P}(\mu, y, t). \quad (\text{D4})$$

This function \mathcal{E} satisfies the evolution equation

$$\frac{\partial \mathcal{E}}{\partial t} = \frac{\partial^2 \mathcal{E}}{\partial x^2} - \lambda(x-1)\Theta(x-1)\mathcal{E} - \lambda \int_{\max(1,x)}^{x+1} dy \mathcal{E}(\mu, y) - 2\mu \frac{\partial \mathcal{E}}{\partial x} + \mu^2 \mathcal{E} \equiv \mathcal{L}_\mu \mathcal{E}, \quad (\text{D5})$$

as it follows from (D1). The boundary condition is deduced from Eq. (D2) to yield

$$\frac{\partial^2 \mathcal{E}}{\partial x^2}(\mu, 0) - \mu \frac{\partial \mathcal{E}}{\partial x}(\mu, 0) = 0. \quad (\text{D6})$$

We observe that equation (D5) is very similar to equations (36a)–(36b) satisfied by the cumulative probability $E(x, t)$, the only difference being in the terms containing μ and μ^2 . The differential operator \mathcal{L}_μ that governs the evolution

of \mathcal{E} is a deformation with parameter μ of the evolution operator \mathcal{L}_0 for E . The long time limit of \mathcal{E} will be given by the dominant eigenvector which corresponds to the largest eigenvalue $U(\mu)$ of \mathcal{L}_μ . We denote $E_\mu(x)$ this dominant eigenvector. It satisfies

$$(U(\mu) - \mu^2) E_\mu = \frac{d^2 E_\mu}{dx^2} - \lambda(x-1)\Theta(x-1)E_\mu - \lambda \int_{\max(1,x)}^{x+1} dy E_\mu(y) - 2\mu \frac{dE_\mu}{dx}. \quad (\text{D7})$$

The boundary condition (D6) becomes

$$E_\mu''(0) = \mu E_\mu'(0), \quad (\text{D8})$$

where the prime denotes the derivative with respect to x . We also normalize $E_\mu(0) = 1$, which is an overall constant that does not affect the final result. We emphasize that this situation is perfectly analogous to the discrete case where the Markov operator $\mathbb{M}(0)$ was μ -deformed into $\mathbb{M}(\mu)$ [see Eq. (26)] and where the dominant eigenvalue allowed us to determine the cumulant generating function.

For $x \geq 1$, we obtain, using again the Laplace method [27, 28], an integral representation for $E_\mu(x)$, which assumes a form analogous to the one found in Eq. (40)

$$\begin{aligned} E_\mu(x) &= A_\mu \int_0^\infty dw C_\mu(w) C_\mu(w, x) \\ C_\mu(w) &= \exp\left(\int_0^w dv \frac{\cos v - 1}{v} - \frac{\mu}{\lambda} w^2\right) \\ C_\mu(w, x) &= \cos[w(x-1) + W_\mu] \\ W_\mu(w) &= W(w) + \frac{U(\mu) - \mu^2}{\lambda} w = \frac{w^3}{3\lambda} + \int_0^w dv \frac{\sin v}{v} + \frac{U(\mu) - \mu^2}{\lambda} w. \end{aligned} \quad (\text{D9})$$

We shall write W_μ instead of $W_\mu(w)$ in equations below. Note that for $\mu = 0$ we recover the expressions in Eq. (41). The constant A_μ is yet to be determined.

In the $0 \leq x \leq 1$ region, the solution is given by

$$E_\mu(x) = \frac{e^{r_+x} + e^{r_-x}}{2} - B_\mu \frac{e^{r_+x} - e^{r_-x}}{r_+ - r_-} - \lambda A_\mu \int_0^\infty dw C_\mu(w) \Phi_\mu(w, x) \quad (\text{D10})$$

with $r_\pm \equiv r_\pm(\mu) = \mu \pm \sqrt{U(\mu)}$ and

$$\begin{aligned} \Phi_\mu(w, x) &= \frac{w^2 - r_+ r_-}{w(r_+^2 + w^2)(r_-^2 + w^2)} \sin(wx + W_\mu) - \frac{2\mu}{(r_+^2 + w^2)(r_-^2 + w^2)} \cos(wx + W_\mu) \\ &+ \frac{\sin W_\mu}{w(r_+ - r_-)} \left[\frac{w^2 e^{r_+x}}{r_+(r_+^2 + w^2)} - \frac{w^2 e^{r_-x}}{r_-(r_-^2 + w^2)} + \frac{1}{r_-} - \frac{1}{r_+} \right] \\ &- \frac{\cos W_\mu}{r_+ - r_-} \left(\frac{e^{r_+x}}{r_+^2 + w^2} - \frac{e^{r_-x}}{r_-^2 + w^2} \right) \end{aligned} \quad (\text{D11})$$

Note again the similarity of structure between these equations and (43)–(44).

The constants A_μ and B_μ can be determined by taking into account that $E_\mu(x)$ and its derivative are continuous at $x = 1$. These constraints lead to

$$\begin{aligned} A_\mu J_{1,\mu} &= \frac{e^{r_+} + e^{r_-}}{2} - B_\mu \frac{e^{r_+} - e^{r_-}}{r_+ - r_-} \\ A_\mu J_{2,\mu} &= B_\mu \frac{r_+ e^{r_+} - r_- e^{r_-}}{r_+ - r_-} - \frac{r_+ e^{r_+} + r_- e^{r_-}}{2} \end{aligned} \quad (\text{D12})$$

where we have used shorthand notation

$$J_{p,\mu} = \int_0^\infty dw \mathcal{W}_{p,\mu}(w) C_\mu(w), \quad p = 1, 2$$

and

$$\begin{aligned} \mathcal{W}_{1,\mu}(w) &= \cos W_\mu(w) + \lambda \Phi_\mu(w, 1) \\ \mathcal{W}_{2,\mu}(w) &= w \sin W_\mu(w) - \lambda \left. \frac{\partial \Phi_\mu(w, x)}{\partial x} \right|_{x=1} \end{aligned}$$

Equations (D9)–(D12) determine the eigenfunction $E_\mu(x)$ in terms of the eigenvalue $U(\mu)$. For $\mu = 0$, $U(0) = 0$ and it can be verified that $E_\mu(x)$ is identical to $E(x)$ given by Eqs. (45)–(48).

The maximal eigenvalue $U(\mu)$ is implicitly determined by the self-consistent equation obtained by substituting $x = 0$ into Eq. (D7), imposing the boundary condition (D8), and using the normalization $E_\mu(0) = 1$. One gets

$$U(\mu) = \mu^2 - \mu E'_\mu(0). \quad (\text{D13})$$

Using relation $\left. \frac{\partial \Phi_\mu(w, x)}{\partial x} \right|_{x=0} = 0$ [which can be deduced from (D12)] and specializing Eq. (D10) to $x = 0$ we find $E'_\mu(0) = \mu - B_\mu$. Inserting this into (D13) we simplify it to

$$U(\mu) = \mu B_\mu. \quad (\text{D14})$$

Solving (D12) and comparing with (D14) we arrive at an implicit expression for the dominant eigenvalue $U(\mu)$,

$$U(\mu) = \mu \left(\frac{r_+ - r_-}{2} \right) \frac{(r_+ e^{r_+} + r_- e^{r_-}) J_{1,\mu} + (e^{r_+} + e^{r_-}) J_{2,\mu}}{(r_+ e^{r_+} - r_- e^{r_-}) J_{1,\mu} + (e^{r_+} - e^{r_-}) J_{2,\mu}},$$

which, using that $r_+ - r_- = 2\sqrt{U(\mu)}$, can be rewritten as

$$U(\mu) = \left[\mu \frac{(r_+ e^{r_+} + r_- e^{r_-}) J_{1,\mu} + (e^{r_+} + e^{r_-}) J_{2,\mu}}{(r_+ e^{r_+} - r_- e^{r_-}) J_{1,\mu} + (e^{r_+} - e^{r_-}) J_{2,\mu}} \right]^2. \quad (\text{D15})$$

We know from Eq. (28) that $U(\mu)$ generates the cumulants of L in the long time limit: $U(\mu) = \mu v + \mu^2 \mathcal{D} + \dots$. Due to the presence of the overall factor μ in Eq. (D15), we observe that the expansion of $U(\mu)$ with respect to μ can be generated order by order in a self-consistent manner. At lowest order, taking the limit $\mu = 0$ on the right-hand side of Eq. (D15), we retrieve the formula (49) for the velocity v . At the next order, retaining the terms linear in μ in r_+ , r_- , $\mathcal{W}_{1,\mu}$, $\mathcal{W}_{2,\mu}$ and C_μ (and substituting $U(\mu) \rightarrow \mu v$) we obtain a formula for the diffusion constant \mathcal{D} :

$$\mathcal{D} = 1 - v + \frac{1}{3}v^3 + \frac{\Delta_2 - v(\Delta_1 + \Delta_2)}{\int_0^\infty dw [\mathcal{W}_1(w) + \mathcal{W}_2(w)] C(w)} \quad (\text{D16})$$

with

$$\begin{aligned} \Delta_1 &= \int_0^\infty dw [\mathcal{W}_1(w) \delta C(w) + \delta \mathcal{W}_1(w) C(w)] \\ \Delta_2 &= \int_0^\infty dw [\mathcal{W}_2(w) \delta C(w) + \delta \mathcal{W}_2(w) C(w)] \end{aligned}$$

The functions $\delta C(w)$, $\delta \mathcal{W}_1(w)$ and $\delta \mathcal{W}_2(w)$ represent the first order derivatives of the functions $C(w)$, $\mathcal{W}_1(w)$ and $\mathcal{W}_2(w)$ with respect to the parameter μ . For instance, $\delta C(w) = \left. \frac{\partial C_\mu(w)}{\partial \mu} \right|_{\mu=0}$ and its explicit expression reads

$$\delta C(w) = -\frac{w^2}{\lambda} C(w).$$

The explicit expressions for $\delta \mathcal{W}_1(w)$ and $\delta \mathcal{W}_2(w)$ are quite cumbersome

$$\begin{aligned} \delta \mathcal{W}_1(w) &= -\frac{v}{\lambda} w \sin W + \frac{\lambda}{w} \left\{ -\frac{v}{w^4} \sin(w+W) + \sin W \left(\frac{1}{3} + \frac{v}{24} + \frac{v}{\lambda w} - \frac{2+v/2}{w^2} + \frac{v}{w^4} \right) \right. \\ &\quad \left. + \cos(w+W) \left(\frac{v}{\lambda w^2} - \frac{2}{w^3} \right) + \cos W \left(\frac{v}{2\lambda} - \frac{1+v/6}{w} - \frac{v}{\lambda w^2} + \frac{2+v}{w^3} \right) \right\}, \\ \delta \mathcal{W}_2(w) &= \frac{v}{\lambda} w^2 \cos W - \frac{\lambda}{w} \left\{ \sin(w+W) \left(-\frac{v}{\lambda w} + \frac{2}{w^2} \right) + \sin W \left(1 + \frac{v}{6} + \frac{v}{\lambda w} - \frac{2+v}{w^2} \right) \right. \\ &\quad \left. - \frac{v}{w^3} \cos(w+W) + \cos W \left(\frac{v}{\lambda} - \frac{2+v/2}{w} + \frac{v}{w^3} \right) \right\}. \end{aligned}$$

These formulas can be used to establish the limiting behavior of the diffusion constant when λ is very small or very large [see Eqs (57) and (58)].

[1] J. Howard, *Mechanics of Motor Proteins and the Cytoskeleton* (Sinauer Associates, Sunderland MA, 2001).

- [2] B. Alberts, A. Johnson, J. Lewis, M. Raff, K. Roberts and P. Walter, *Molecular Biology of the Cell* (Garland Publishing, New York, 2002).
- [3] R. P. Feynman, R. Leighton and M. Sands, *The Feynman Lectures on Physics, Vol. 1* (Addison-Wesley, San Francisco, 1963).
- [4] S. M. Simon, C. S. Peskin and G. F. Oster, Proc. Natl. Acad. Sci. **89**, 3770 (1992).
- [5] C. S. Peskin, G. M. Odell, and G. F. Oster, Biophys. J. **65**, 316 (1993); T. C. Elston and C. S. Peskin, SIAM J. Appl. Math. **60**, 842 (2000); T. C. Elston, D. You, and C. S. Peskin, SIAM J. Appl. Math. **61**, 776 (2000).
- [6] P. Nelson, *Biological Physics. Energy, Information, Life* (W. H. Freeman and Company, New York, 2004).
- [7] D. K. Lubensky and D. R. Nelson, Biophys. J. **77**, 1824 (1999).
- [8] T. C. Elston, Biophys. J. **79**, 2235 (2000); *ibid* **82**, 1239 (2002).
- [9] W. Liebermeister, T. A. Rapoport and R. Heinrich, J. Mol. Biol. **305**, 643 (2001).
- [10] R. Zandi, D. Reguera, J. Rudnick J, and W. M. Gelbart, Proc. Natl. Acad. Sci. **100**, 8649 (2003).
- [11] T. Ambjörnsson and R. Metzler, Phys. Biol. **1**, 77 (2004); T. Ambjörnsson, M. A. Lomholt and R. Metzler, J. Phys.: Cond. Matter **17**, S3945 (2005).
- [12] M. R. D'Orsogna, T. Chou, and T. Antal, J. Phys. A **40**, 5575 (2007).
- [13] H. Salman, D. Zbaida, Y. Rabin, D. Chatenay, and M. Elbaum, Proc. Natl. Acad. Sci. **98**, 7247 (2001).
- [14] J. W. Evans, Rev. Mod. Phys. **65**, 1281 (1993).
- [15] P. L. Krapivsky, S. Redner and E. Ben-Naim, *A Kinetic View of Statistical Physics* (Cambridge: Cambridge University Press, 2010).
- [16] M. Abramowitz and I. A. Stegun, *Handbook of Mathematical Functions* (Dover Publications Inc., 1965).
- [17] J. D. Watson, *A Treatise on the Theory of Bessel Functions* (Cambridge: Cambridge University Press, 1995).
- [18] See [17], section 8-42, equation (7). Note that the polynomials $B_m(x)$ that appear in that equation, and in our equation (18), have no relation with Bernoulli polynomials which are also denoted $B_m(x)$.
- [19] B. Derrida, M. R. Evans and K. Mallick, J. Stat. Phys. **79**, 833 (1995).
- [20] B. Derrida and K. Mallick, J. Phys. A **30**, 3817 (1997).
- [21] T. Antal, P. L. Krapivsky, and K. Mallick, J. Stat. Mech. P08027 (2007).
- [22] J. Mai, I. M. Sokolov, and A. Blumen, Phys. Rev. E **64**, 011102 (2001).
- [23] T. Antal and P. L. Krapivsky, Phys. Rev. E **72**, 046104 (2005); A. Yu. Morozov, E. Pronina, A. B. Kolomeisky, and M. N. Artyomov, Phys. Rev. E **75**, 031910 (2007).
- [24] N. G. Van Kampen, *Stochastic Processes in Physics and Chemistry* (North-Holland, 3rd edition, 2007).
- [25] A. Dembo and O. Zeitouni, *Large Deviations Techniques and Applications*, 2nd ed (New York : Springer, 1998).
- [26] It seems plausible that the difference-differential analog (37a)–(37b) of the Airy equation should play a role in various adsorption models.
- [27] L. D. Landau and E. M. Lifshitz, *Quantum Mechanics* (Butterworth-Heinemann, 1981).
- [28] E. J. B. Goursat, *A Course in Mathematical Analysis*, vol. 2 (Dover, New York, 1959).
- [29] E. W. Montroll and M. F. Shlesinger, *On the Wonderful World of Random Walks*, in: *Studies in Statistical Mechanics Vol. XI*, J. L. Lebowitz and E. W. Montroll Eds. (Elsevier, North-Holland, 1984).
- [30] S. Redner, *A Guide to First-Passage Processes* (Cambridge University Press, June 2007).
- [31] F. Jülicher, A. Ajdari and J. Prost, Rev. Mod. Phys. **69**, 1269 (1997).
- [32] P. Reimann, Phys. Rep. **361**, 57 (2002).
- [33] Y. Kafri, D. K. Lubensky and D. R. Nelson, Biophys. J. **86**, 3373 (2004).
- [34] A. Lau, D. Lacoste and K. Mallick, Phys. Rev. Lett. **99**, 158102 (2007).
- [35] C. de Duve, *A Guided Tour of the Living Cell* (W. H. Freeman and Company, June 1984).
- [36] J. Kurchan, J. Phys. A: Math. Gen. **31**, 3719 (1998).
- [37] J. L. Lebowitz and H. Spohn, J. Stat. Phys. **95**, 333 (1999).
- [38] K. E. P. Sugden, M. R. Evans, W. C. K. Poon, and N. D. Read, Phys. Rev. E **75**, 031909 (2007).